LANGMUIR

pubs.acs.org/Langmuir Article

Demetalation of Surface Porphyrins at the Solid–Liquid Interface

Cynthia C. Fernández, Matthias Franke, Hans-Peter Steinrück, Ole Lytken, and Federico J. Williams*

Cite This: *Langmuir* 2021, 37, 852–857 Read Online

ACCESS | Metrics & More | Article Recommendations | Supporting Information

ABSTRACT: Understanding the factors that control the demetalation of surface porphyrins at the solid–liquid interface is important as the molecular properties of porphyrins are largely determined by their metal centers. In this work, we used X-ray photoelectron spectroscopy (XPS) to follow the demetalation of Zn and Cd tetraphenylporphyrin molecules (ZnTPP and CdTPP) adsorbed as three-monolayer-thin multilayer films on Au(111), by exposing the molecular layers to acidic aqueous solutions. We found that porphyrin molecules at the solid–liquid interface are less prone to lose their metal center than molecules in solution. We propose that this behavior is due to either the incoming protons provided by the solution or the outgoing metal ion having to pass through the hydrophobic porphyrin multilayers where they cannot be solvated. Our results are relevant for the design of molecular devices based on porphyrin molecules adsorbed on solid surfaces.

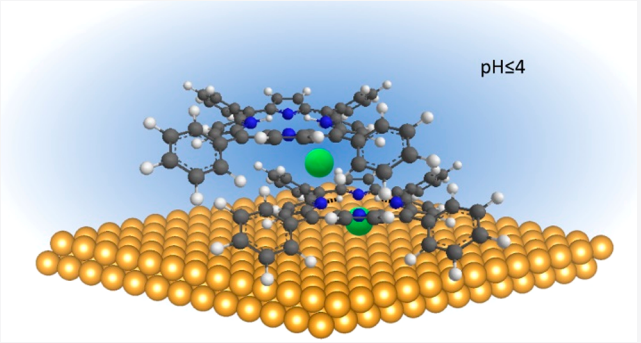

INTRODUCTION

Porphyrins are a group of tetrapyrroles that play a key role in biological processes such as oxygen transport and storage,[1] electron transport,[2] and photosynthesis.[3] Porphyrins have a strong absorption in the UV–visible region as well as excellent photostability. The nitrogen atoms of the pyrrolic rings form a reactive core which can incorporate different metallic centers, generating a rich coordination chemistry. This allows for tuning their chemical, optical, electronic, and magnetic properties and consequently their functionality. For this reason, porphyrins attached to surfaces constitute the basic building blocks of a variety of molecular devices including solar cells,[4,5] organic light-emitting devices,[6] sensors,[7,8] catalysts,[9] and molecular electronic devices.[10] Consequently, there has been a great research effort undertaken during the recent past to understand the interaction of porphyrin molecules with solid surfaces.[11,12]

Porphyrin molecules adsorbed on surfaces can undergo chemical reactions involving the central cavity. In the free-base form this central cavity contains two protons which can be exchanged with codeposited metal atoms[13,14] or with metal ions from solution,[15−17] resulting in a metalloporphyrin. In a process known as self-metalation, porphyrins adsorbed on metal or oxide surfaces can be metalated with substrate atoms.[18,19] Furthermore, the iminic nitrogen atoms at the central cavity can protonate with surface hydroxyl groups, giving rise to protonated molecules.[20] Metalated porphyrin molecules adsorbed on surfaces can also undergo a transmetalation reaction in which the central metal ion is replaced by another metal atom coadsorbed on the surface or from solution.[21,22] The central metal ion can also be replaced with two protons in a reverse metalation reaction called demetalation. This demetalation reaction has been observed under reduction conditions when porphyrin molecules are adsorbed on metal electrodes.[23,24] However, it was not yet observed when exposing the surface molecules to acidic solutions.[22]

In solution, metal porphyrins can demetalate under acidic conditions.[25] Porphyrin complexes with alkali and alkaline earths metals are easily demetalated in mildly acidic solutions, while porphyrins with transition metals with partially filled *d* orbitals are more stable against demetalation. Zn^{2+} and Cd^{2+} ions have a d^{10} electron configuration, and porphyrins complexed with these metals do therefore not show ligand-field stabilization, making them less stable than other transition-metal porphyrin complexes.[26] Furthermore, Zn^{2+} ions fit well into the molecular central cavity, whereas the larger Cd^{2+} ions do not.[27] As a result, Zn^{2+} porphyrins are more stable toward demetalation than Cd^{2+} porphyrins.[28]

In this work we studied the demetalation of porphyrin molecules adsorbed on Au(111) single-crystal surfaces exposed to acidic aqueous solutions. Specifically, we investigated the demetalation of multilayers of Zn(II) and Cd(II) *meso*-tetraphenylporphyrin molecules (ZnTPP and CdTPP) using X-ray photoelectron spectroscopy (XPS). Our results shed new

Received: November 4, 2020
Revised: December 23, 2020
Published: January 5, 2021

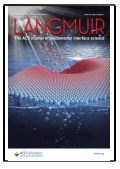

https://dx.doi.org/10.1021/acs.langmuir.0c03197
Langmuir 2021, 37, 852–857

light on the stability of surface porphyrins toward demetalation in relation to solution porphyrins.

EXPERIMENTAL SECTION

Materials. Surface measurements were carried out using a Au(111) single crystal (MaTecK GmbH). *meso*-Tetraphenylporphyrin (2HTPP) and zinc(II) *meso*-tetraphenylporphyrin (ZnTPP) were purchased from Sigma-Aldrich, and cadmium(II) *meso*-tetraphenylporphyrin (CdTPP) was purchased from Por-Lab GmbH; all were used without further purification.

Samples Preparation. The Au(111) single crystal was cleaned by several Ar^+ sputtering and annealing cycles until only Au-related signals were detected by XPS. ZnTPP layers on Au(111) were prepared by thermal evaporation in UHV using a Knudsen cell. Evaporation of CdTPP, however, resulted in mixed layers containing both free-base and metalated porphyrins. After each deposition the degree of metalated molecules increased, but free-base molecules were always present. Free-base 2HTPP is expected to have a lower sublimation temperature than CdTPP, meaning a small concentration of 2HTPP in the CdTPP powder will result in a significantly higher concentration in the evaporated layers. To avoid this we decided to instead deposit the CdTPP layers on Au(111) from methanolic solution. 2HTPP and ZnTPP monolayers (ML) on Au(111) were prepared by multilayer deposition and subsequent annealing above the multilayer desorption temperature (500 K). CdTPP multi- and monolayers were deposited by adjusting the solution deposition procedure. Multilayer coverage was estimated by the attenuation of the substrate XPS signal as discussed elsewhere.[29] All the experiments that required contact between the substrate and a solution were carried out under an argon atmosphere in a liquid reactor attached to the UHV chamber, preventing contact with the laboratory atmosphere (fully described elsewhere).[30] After contact with the solution, the substrate was rinsed with ultrapure water, dried with argon, and, after pumping down, moved back into UHV for measurement.

UV−Vis Spectroscopy. Absorption spectra were measured using a Shimadzu UV-3600 UV−vis spectrophotometer. Spectra were normalized with respect to the spectra of blank solutions. Ten micromolar ZnTPP and CdTPP methanolic solutions were employed for reference measurements. Aqueous pH = 1 solutions with a porphyrin concentration of 10 μM were created using trifluoroacetic acid (TFA). To increase the solubility of 2HTPP, pH = 4 solutions were prepared by adding TFA to a solution of 10% MeOH in H_2O.

X-ray Photoelectron Spectroscopy. XPS measurements were performed at room temperature in a UHV chamber with a base pressure below 5×10^{-10} mbar using a hemispherical SPECS electron energy analyzer and a nine-channeltron detector. All spectra were acquired using a monochromatic Al Kα X-ray source with a photon energy of 1486.6 eV operated at 15 kV and 20 mA and an electron detection angle of 20° with respect to the surface normal. The pass energy of the analyzer was 20 eV, and the energy step was 0.1 eV. All spectra are referenced to the Au $4f_{7/2}$ peak at 84 eV.

RESULTS AND DISCUSSION

Figure 1 shows the chemical reactions that could take place as the pH is lowered. Increasing the concentration of protons in solution will shift the equilibriums in Figure 1 to the right, first toward demetalation, where the metal cation is replaced by two protons. As the concentration of protons is increased further, the iminic nitrogen atoms will become protonated, creating a porphyrin diacid. These reactions can be followed in solution using UV−vis spectroscopy as the free-base, metallo-, and protonated porphyrin species have intense Soret bands (350 to 500 nm) at different positions and as there are important differences in the number and the relative energies of the $\pi \rightarrow \pi^*$ transitions that give rise to the Q bands (500 to 750 nm).[31] The spectrum of free-base *meso*-tetraphenylporphyrin has four

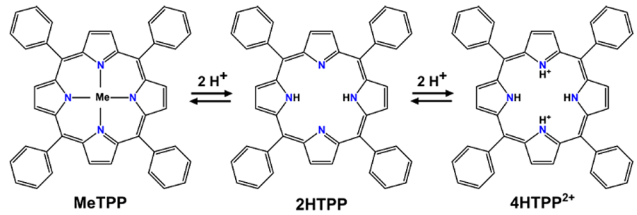

Figure 1. Chemical structures of metalated *meso*-tetraphenylporphyrin (MeTPP), free-base *meso*-tetraphenylporphyrin (2HTPP), and diprotonated *meso*-tetraphenylporphyrin ($4HTPP^{2+}$).

Q bands, but when the porphyrin molecules coordinate a metal ion, there is a change in symmetry from D_{2h} to D_{4h}, reducing the number of Q bands from four to two.[32] The fully protonated diacid form also has D_{4h} symmetry and therefore also two Q bands, but at different positions and with a different intensity ratio.[33]

Figure 2 shows the main species present in ZnTPP and CdTPP solutions at pH = 4 and pH = 1. Figure 2a depicts the UV−visible absorption reference spectra corresponding to ZnTPP (black line), 2HTPP (red line), and $4HTPP^{2+}$ (blue line). As expected, ZnTPP shows two Q bands at 555 and 595 nm,[34] 2HTPP shows four Q bands at 518, 551, 593, and 649 nm,[34,35] and $4HTPP^{2+}$ shows two Q bands at 600 and 652 nm.[33] Note that the broadening of the Soret band in the spectrum of 2HTPP is due to aggregation by stacking which is caused by the poor solubility of the molecule.[36] Figures 2b and 2c show UV−visible absorption spectra of ZnTPP and CdTPP methanolic solutions (black line) and of solutions at pH = 4 (red line) and pH = 1 (blue line). Clearly at pH = 4 both molecules are demetalated as the main species present in solution is 2HTPP. Note that we cannot rule out the presence of small quantities of ZnTPP at pH = 4.

Furthermore, at pH = 1 both molecules are present in the diprotonated diacid form $4HTPP^{2+}$. However, as we shall discuss below, when ZnTPP and CdTPP are adsorbed on surfaces their behavior is different.

X-ray photoelectron spectroscopy has been extensively used to study the metalation reaction of porphyrin molecules adsorbed on metal surfaces as the insertion of the metal center into the porphyrin core can be monitored following changes in the N 1s spectrum.[37] Free-base porphyrin molecules contain four nitrogen atoms, namely, two aminic/pyrrolic (−NH−) and two iminic (−N═). These nitrogen atoms are chemically nonequivalent and give rise to two different photoemission peaks in the N 1s spectrum, separated by approximately 2 eV.[38] In the metalated molecules, however, the four nitrogen atoms are coordinated equally to the central ion and give rise to only one peak in the N 1s region. Figure 3 shows the N 1s spectra corresponding to 1 ML of 2HTPP, 1.1 ML of CdTPP, and 1 ML of ZnTPP molecules adsorbed on Au(111). The N 1s spectrum of 2HTPP shows the two expected components at 399.3 and 397.8 eV in a 1:1 ratio, corresponding to the aminic (−NH−) and iminic (−N═) nitrogen atoms in the free-base porphyrin, respectively. ZnTPP molecules show a single peak at 398 eV. The N 1s spectrum corresponding to CdTPP shows a main peak at 397.6 eV (red curve) that corresponds to the metalated CdTPP molecules; however, it also shows one small component at 399.6 eV. This extra component is mainly due to free-base porphyrin molecules that are codeposited with CdTPP as the starting chemical contained small quantities of 2HTPP (see the Experimental Section). Note that we cannot

https://dx.doi.org/10.1021/acs.langmuir.0c03197
Langmuir 2021, 37, 852−857

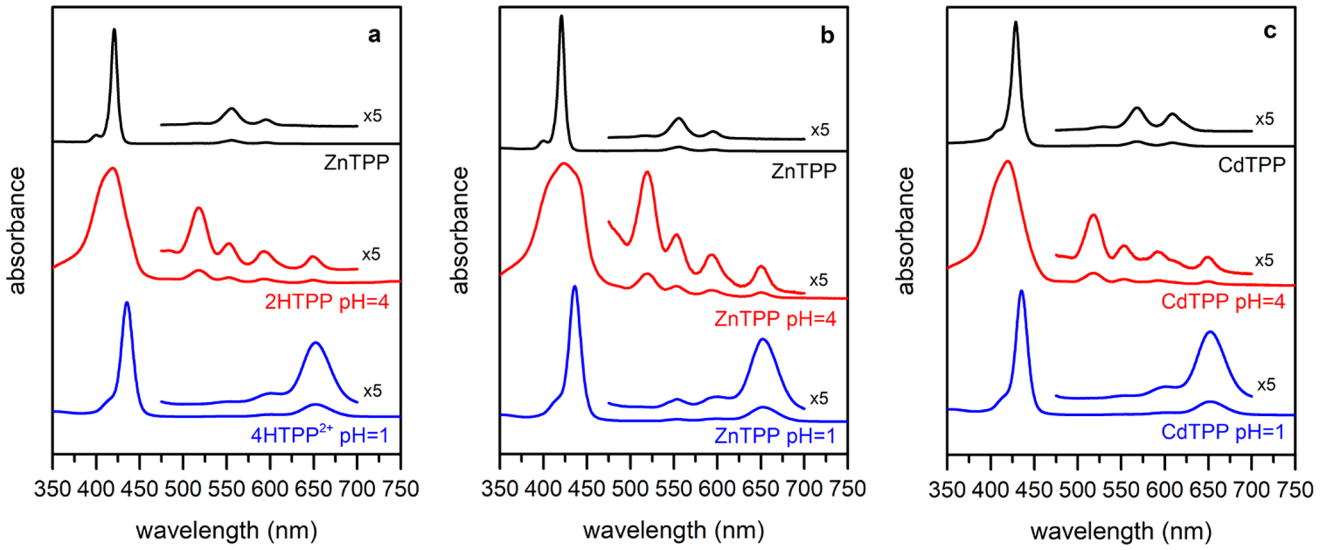

Figure 2. UV−visible absorption spectra of dissolved ZnTPP and CdTPP as a function of pH, compared to reference spectra of ZnTPP, 2HTPP, and $4HTPP^{2+}$. (a) ZnTPP methanolic solution (black line), 2HTPP at pH = 4 (red line), and $4HTPP^{2+}$ at pH = 1 (blue line), (b) ZnTPP, and (c) CdTPP methanolic solutions (black lines), at pH = 4 (red lines) and at pH = 1 (blue lines), respectively.

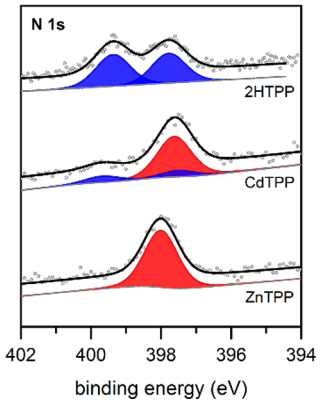

Figure 3. N 1s XP spectra of 1 ML of 2HTPP, 1.1 ML of CdTPP and 1 ML of ZnTPP adsorbed on Au(111).

rule out codeposition of N-containing impurities from solution that should give a peak at around the same position.[15,22,39] However, given that the sensitivity-factor-corrected total C/N XPS ratio is 11.2:1 in agreement with the 11:1 molecular stoichiometry, we can confidently assign the 399.6 eV component to 2HTPP molecules (blue curve). Thus, we introduced an extra component (blue curve) with the same intensity at 397.5 eV to account for the different N chemical environments present in the molecule.

Figure 4 shows the N 1s, Zn $2p_{3/2}$, C 1s, and Au 4f spectra corresponding to the initial Au(111) surface and to 3.2 ML of ZnTPP adsorbed on Au(111) before and after exposing the layers to a pH = 1 solution for 30 min. Initially, 3.2 ML of ZnTPP shows a single N 1s peak at 398 eV accompanied by a shakeup satellite peak at 401 eV and a single Zn $2p_{3/2}$ peak at 1021.6 eV. The sensitivity-factor-corrected N/Zn XPS ratio is 4:1.1, in agreement with the 4:1 molecular stoichiometry. After exposure to the acidic solution, the N 1s spectrum remains essentially constant, except for a new peak at 399.7 eV. This additional peak could be due to 2HTPP molecules and/or to nitrogen-containing impurities.[15,22,39] However, given that the total area of the N 1s peak remains constant, we assign the peak at 399.7 eV to mainly 2HTPP molecules and therefore

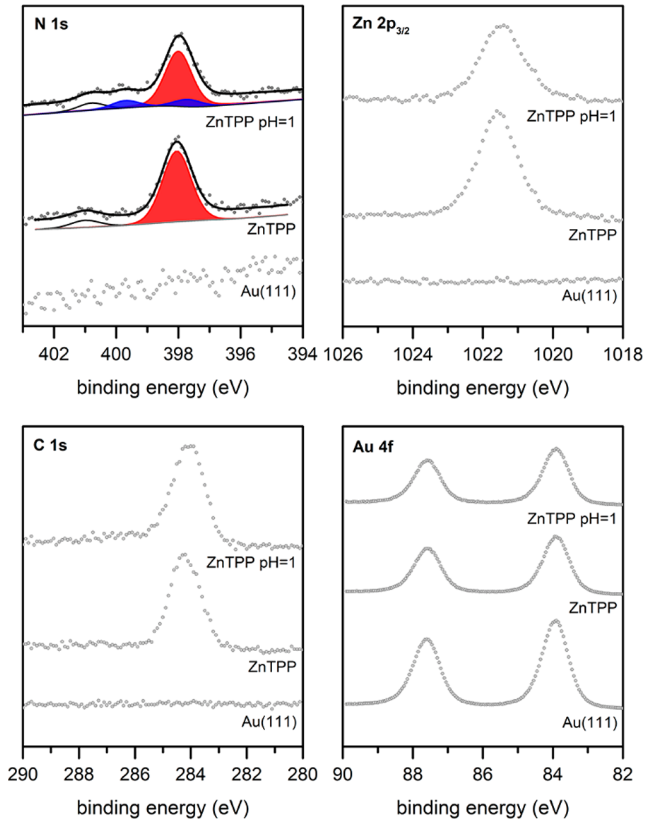

Figure 4. N 1s, Zn $2p_{3/2}$, C 1s, and Au 4f XP spectra corresponding to 3.2 ML of ZnTPP adsorbed on Au(111) before and after being exposed for 30 min to a pH = 1 aqueous solution.

added a new peak at 397.8 eV with the same intensity to account for the different N environments in the molecule. The area of the Zn $2p_{3/2}$ peak decreases by 21% after exposure to the acidic solution, suggesting that only 21% of the molecules suffered demetalation. Note that the area of the main N 1s peak at 398 eV (red curve) is in line with the amount of Zn left on the surface. The area of the C 1s peak increases only slightly

https://dx.doi.org/10.1021/acs.langmuir.0c03197
Langmuir 2021, 37, 852−857

and the Au 4f peak remains essentially constant after exposure to the pH = 1 solution. This indicates that only a very small number of unwanted species remain on the surface after exposure to the acidic solution. In the past, we have carried out similar experiments involving 1 ML of ZnTPP adsorbed on Au(111) which indicated no demetalation,[22] in line with the present multilayer experiments that show only slight demetalation. This is in stark contrast to the behavior of dissolved ZnTPP that indicates full demetalation at pH = 1 (see Figure 2). We explain this difference as follows. Although the precise details of the metalloporphyrin demetalation mechanism is a matter of current debate,[40] we can assume that during demetalation protons attack the central cavity from one side while the metal ions exit from the other side. In solution, solvent molecules are present on both sides of the cavity and stabilize both the incoming protons and the outgoing metal ions, reducing the activation energy barrier of the reaction. For adsorbed molecules, however, only one side of the cavity is accessible to solvent molecules. For demetalation, this means that either the incoming protons provided by the solution or the outgoing metal ion would have to pass through the hydrophobic porphyrin multilayers, which decreases the rate of demetalation. Furthermore, in our experiments, the crystal is rinsed with ultrapure water after exposing the porphyrin layers to the pH = 1 solution (note that we do not have evidence on the presence of water in the film after rinsing). This causes most of the displaced Zn^{2+} to be reinserted into the molecular central cavity. Note that some Zn^{2+} might be washed away from the layers, leading to the observation of a small degree of demetalation. This situation is different in the case of CdTPP as the larger Cd^{2+} cation cannot easily metalate the molecule back due to its size.

Figure 5 shows N 1s, Cd 3d, C 1s, and Au 4f spectra corresponding to the initial Au(111) surface and to 2.8 ML of CdTPP before and after exposure to a pH = 4 solution for 30 min. The Cd 3d spectrum corresponding to the initial CdTPP layer shows the expected $3d_{5/2}$ and $3d_{3/2}$ doublet at 404.3 and 411.1 eV in a 3:2 ratio. The respective N 1s spectrum shows a main peak at 397.7 eV (red curve) corresponding to CdTPP and one small component at 399.7 eV (blue curve). As discussed above (see Figure 3) this latter component is assigned to codeposited 2HTPP free-base molecules present in the starting chemical, and thus, an additional peak with the same intensity at 397.5 eV (blue curve) is needed to account for the different N environments in the molecule. Note that the sensitivity-factor-corrected total C/N XPS ratio is 11.1:1, in agreement with the 11:1 molecular stoichiometry. The C 1s and Au 4f peak intensities remain constant after exposing the CdTPP multilayers to the pH = 4 solution, indicating that no molecules are lost and that no impurities are deposited on the surface. However, changes are observed in both the Cd 3d and N 1s regions after exposure to the pH = 4 solution. The N 1s intensity remains constant but its shape changes drastically, showing a large increase in the contributions due to free-base molecules. The observed increase indicates that 74% of the CdTPP molecules are demetalated. On the other hand, the intensity of the Cd 3d signal decreases by 57% and both peaks broaden. Therefore, the Cd 3d signal could be fitted with two doublets, one due to CdTPP molecules that remained metalated after exposure to the acidic solution and with an intensity equal to 26% of the original signal (404.3 and 411.1 eV red curves) and a new doublet at lower binding energy (404.0 and 410.7 eV green curves). Note that the Cd 3d

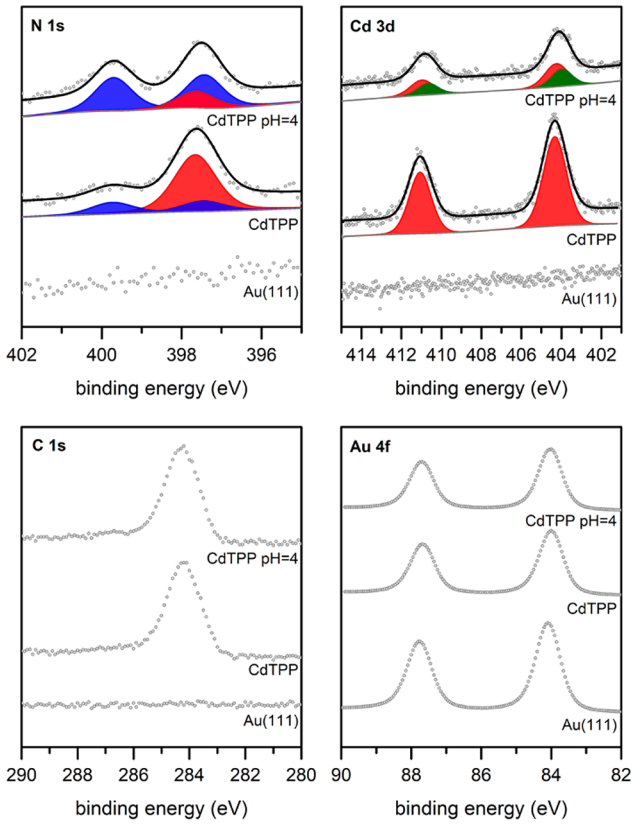

Figure 5. N 1s, Cd 3d, C 1s, and Au 4f XP spectra of 2.8 ML of CdTPP molecules adsorbed on Au (111) before and after being exposed for 30 min to a pH = 4 aqueous solution.

contribution due to CdTPP was fitted by fixing its area to the corresponding N 1s signal. Although Cd^{2+} could form surface alloys with Au(111) single-crystal surfaces after electrochemical reduction,[41] the Cd $3d_{5/2}$ binding energy of the alloy is 405 eV.[42] Thus, in line with the fact that oxidation of Cd causes a negative Cd $3d_{5/2}$ binding energy shift,[43] we assign the 404.0 eV component to displaced Cd^{2+} ions that remained in the molecular layers. Note that the degree of demetalation is larger than that observed for ZnTPP (see Figure 4); however, the demetalation reaction is also inhibited in comparison to the solution behavior (see Figure 2). In this case, rinsing does not cause the reinsertion of Cd^{2+} cations into the porphyrin central cavity as the larger Cd^{2+} cannot metalate the molecule under these conditions and therefore a larger degree of demetalation is observed. Finally, we note that CdTPP monolayers adsorbed on Au(111) also show partial demetalation after a 30 min exposure to a pH = 4 solution (see Figure S1).

Figure 6 shows the N 1s and Cd 3d spectra measured after successive 30 min immersions of 2.8 ML CdTPP adsorbed on Au(111) into pH = 4 solutions. Clearly, each successive exposure to the acidic solution resulted in a decrease in the Cd 3d intensity whereas the total N 1s signal remained constant. Note that the intensity of the C 1s and Au 4f signals also remained constant after each successive immersion (see Figure S2), indicating that no porphyrin molecules are lost from the surface and that no unwanted species are adsorbed. The shape of the N 1s spectra changed with the number of immersions as the nitrogen signal due to the free-base molecules (blue curves) increased. The degree of demetalation after each successive immersion is shown in Figure 7a, indicating that

https://dx.doi.org/10.1021/acs.langmuir.0c03197
Langmuir 2021, 37, 852−857

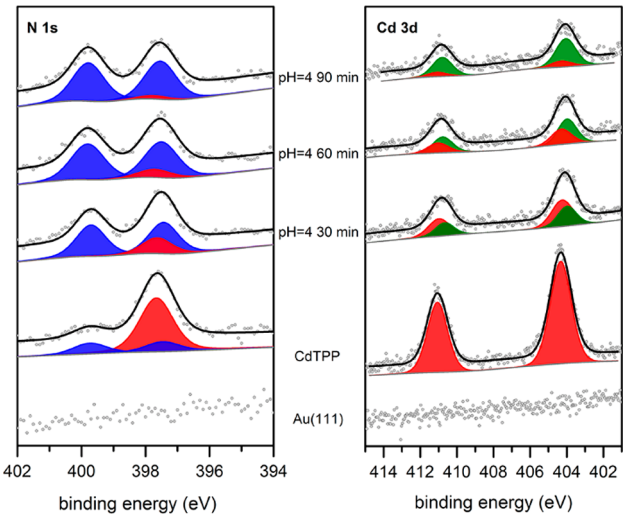

Figure 6. N 1s and Cd 3d XP spectra of 2.8 ML CdTPP molecules adsorbed on the Au(111) before and after being exposed for 30, 60, and 90 min to a pH = 4 aqueous solution.

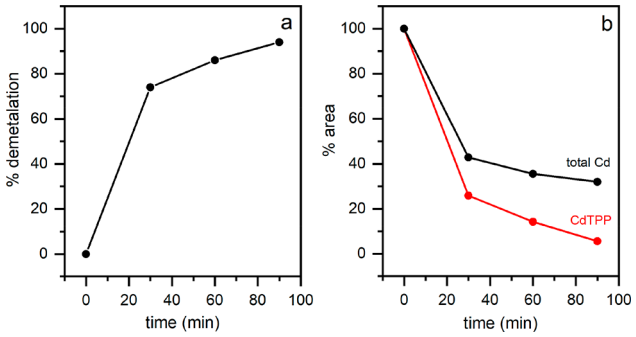

Figure 7. (a) Degree of demetalation and (b) the percentage decrease in the total Cd 3d signal (black curve) and the CdTPP-related Cd 3d signal (red curve) after each successive 30 min immersion of 2.8 ML of CdTPP adsorbed on Au(111) in a pH = 4 solution.

74%, 86%, and 95% of the initial molecules are demetalated after each solution exposure. In parallel, the intensity of the Cd 3d signal decreases after each immersion step. As discussed above, it could be fitted with two doublet components, one due to the CdTPP molecules left on the surface (red curves in Figure 6) and the other due to displaced Cd^{2+} (green curves in Figure 6). Figure 7b shows that the total Cd intensity decreases in a smaller proportion than the CdTPP intensity calculated from the N peak at 397.7 eV (N−Cd). This indicates that as more molecules are demetalated the amount of displaced Cd^{2+} ions in the film increases.

CONCLUSIONS

XPS shows that ZnTPP multilayers adsorbed on Au(111) are slightly demetalated when exposed to pH = 1 solutions, whereas CdTPP mono- and multilayers exhibited a larger degree of demetalation even at pH = 4. In both cases the degree of demetalation is much lower than that observed when the molecules are dissolved in liquid solutions. We propose that demetalation of adsorbed metalloporphyrin molecules is hindered as either the incoming protons provided by the solution or the outgoing metal ion would have to pass through the hydrophobic porphyrin multilayers where they cannot be solvated. Our results are relevant for the design of molecular devices based on porphyrin molecules acting at the solid/liquid interface.

ASSOCIATED CONTENT

Supporting Information

The Supporting Information is available free of charge at https://pubs.acs.org/doi/10.1021/acs.langmuir.0c03197.

Additional XPS data (PDF)

AUTHOR INFORMATION

Corresponding Author

Federico J. Williams − *Departamento de Química Inorgánica, Analítica y Química Física, Facultad de Ciencias Exactas y Naturales and Instituto de Química Física de los Materiales, Medio Ambiente y Energía INQUIMAE, CONICET, Universidad de Buenos Aires, Buenos Aires, Argentina;* orcid.org/0000-0002-6194-2734; Email: fwilliams@qi.fcen.uba.ar

Authors

Cynthia C. Fernández − *Departamento de Química Inorgánica, Analítica y Química Física, Facultad de Ciencias Exactas y Naturales and Instituto de Química Física de los Materiales, Medio Ambiente y Energía INQUIMAE, CONICET, Universidad de Buenos Aires, Buenos Aires, Argentina*

Matthias Franke − *Lehrstuhl für Physikalische Chemie II, Universität Erlangen-Nürnberg, Erlangen, Germany*

Hans-Peter Steinrück − *Lehrstuhl für Physikalische Chemie II, Universität Erlangen-Nürnberg, Erlangen, Germany;* orcid.org/0000-0003-1347-8962

Ole Lytken − *Lehrstuhl für Physikalische Chemie II, Universität Erlangen-Nürnberg, Erlangen, Germany;* orcid.org/0000-0003-0572-0827

Complete contact information is available at: https://pubs.acs.org/10.1021/acs.langmuir.0c03197

Notes

The authors declare no competing financial interest.

ACKNOWLEDGMENTS

C.C.F. acknowledges a scholarship from the Consejo Nacional de Investigaciones Científicas y Técnicas (CONICET). Financial support from the Deutsche Forschungsgemeinschaft (DFG) within the Research Unit FOR 1878 funCOS, of the Agencia Nacional de Promoción de la Investigación, of el Desarrollo Tecnológico y la Innovación (PICT 2018-03276), and of the Universidad de Buenos Aires (UBACyT 20020190100028BA) is acknowledged. F.J.W. thanks DFG for financial funding through a Mercator Fellowship.

REFERENCES

(1) Poulos, T. L. Heme Enzyme Structure and Function. *Chem. Rev.* **2014**, *114* (7), 3919−3962.

(2) Hüttemann, M.; Pecina, P.; Rainbolt, M.; Sanderson, T. H.; Kagan, V. E.; Samavati, L.; Doan, J. W.; Lee, I. The Multiple Functions of Cytochrome c and Their Regulation in Life and Death Decisions of the Mammalian Cell: From Respiration to Apoptosis. *Mitochondrion* **2011**, *11* (3), 369−381.

(3) Borah, K. D.; Bhuyan, J. Magnesium Porphyrins with Relevance to Chlorophylls. *Dalt. Trans.* **2017**, *46* (20), 6497−6509.

(4) Mathew, S.; Yella, A.; Gao, P.; Humphry-Baker, R.; Curchod, B. F. E.; Ashari-Astani, N.; Tavernelli, I.; Rothlisberger, U.; Nazeeruddin,

M. K.; Grätzel, M. Dye-Sensitized Solar Cells with 13% Efficiency Achieved through the Molecular Engineering of Porphyrin Sensitizers. *Nat. Chem.* **2014**, *6* (3), 242−247.
(5) Yella, A.; Lee, H.-W.; Tsao, H. N.; Yi, C.; Chandiran, A. K.; Nazeeruddin, M. K.; Diau, E. W.-G.; Yeh, C.-Y.; Zakeeruddin, S. M.; Grätzel, M. Porphyrin-Sensitized Solar Cells with Cobalt (II/III)-Based Redox Electrolyte Exceed 12% Efficiency. *Science* **2011**, *334* (6056), 629−634.
(6) Zhu, L. J.; Wang, J.; Reng, T. G.; Li, C. Y.; Guo, D. C.; Guo, C. C. Effect of Substituent Groups of Porphyrins on the Electroluminescent Properties of Porphyrin-Doped OLED Devices. *J. Phys. Org. Chem.* **2010**, *23* (3), 190−194.
(7) Ding, Y.; Zhu, W. H.; Xie, Y. Development of Ion Chemosensors Based on Porphyrin Analogues. *Chem. Rev.* **2017**, *117* (4), 2203−2256.
(8) Filippini, D.; Alimelli, A.; Di Natale, C.; Paolesse, R.; D'Amico, A.; Lundström, I. Chemical Sensing with Familiar Devices. *Angew. Chem., Int. Ed.* **2006**, *45* (23), 3800−3803.
(9) Costentin, C.; Dridi, H.; Savéant, J. M. Molecular Catalysis of O2 Reduction by Iron Porphyrins in Water: Heterogeneous versus Homogeneous Pathways. *J. Am. Chem. Soc.* **2015**, *137* (42), 13535−13544.
(10) Jurow, M.; Schuckman, A. E.; Batteas, J. D.; Drain, C. M. Porphyrins as Molecular Electronic Components of Functional Devices. *Coord. Chem. Rev.* **2010**, *254* (19−20), 2297−2310.
(11) Auwärter, W.; Écija, D.; Klappenberger, F.; Barth, J. V. Porphyrins at Interfaces. *Nat. Chem.* **2015**, *7* (2), 105−120.
(12) Gottfried, J. M. Surface Chemistry of Porphyrins and Phthalocyanines. *Surf. Sci. Rep.* **2015**, *70* (3), 259−379.
(13) Shubina, T. E.; Marbach, H.; Flechtner, K.; Kretschmann, A.; Jux, N.; Buchner, F.; Steinrück, H. P.; Clark, T.; Gottfried, J. M. Principle and Mechanism of Direct Porphyrin Metalation: Joint Experimental and Theoretical Investigation. *J. Am. Chem. Soc.* **2007**, *129* (30), 9476−9483.
(14) Gottfried, J. M.; Flechtner, K.; Kretschmann, A.; Lukasczyk, T.; Steinrück, H. P. Direct Synthesis of a Metalloporphyrin Complex on a Surface. *J. Am. Chem. Soc.* **2006**, *128* (17), 5644−5645.
(15) Franke, M.; Marchini, F.; Steinrück, H. P.; Lytken, O.; Williams, F. J. Surface Porphyrins Metalate with Zn Ions from Solution. *J. Phys. Chem. Lett.* **2015**, *6* (23), 4845−4849.
(16) Fernandez, C. C.; Spedalieri, C.; Murgida, D. H.; Williams, F. J. Surface Influence on the Metalation of Porphyrins at the Solid-Liquid Interface. *J. Phys. Chem. C* **2017**, *121* (39), 21324−21332.
(17) Wechsler, D.; Fernández, C. C.; Steinrück, H. P.; Lytken, O.; Williams, F. J. Covalent Anchoring and Interfacial Reactions of Adsorbed Porphyrins on Rutile TiO2(110). *J. Phys. Chem. C* **2018**, *122* (8), 4480−4487.
(18) Diller, K.; Klappenberger, F.; Marschall, M.; Hermann, K.; Nefedov, A.; Wöll, C.; Barth, J. V. Self-Metalation of 2H-Tetraphenylporphyrin on Cu(111): An x-Ray Spectroscopy Study. *J. Chem. Phys.* **2012**, *136* (1), 014705.
(19) Wechsler, D.; Fernández, C. C.; Tariq, Q.; Tsud, N.; Prince, K. C.; Williams, F. J.; Steinrück, H.; Lytken, O. Interfacial Reactions of Tetraphenylporphyrin with Cobalt-Oxide Thin Films. *Chem. - Eur. J.* **2019**, *25* (57), 13197−13201.
(20) Köbl, J.; Wang, T.; Wang, C.; Drost, M.; Tu, F.; Xu, Q.; Ju, H.; Wechsler, D.; Franke, M.; Pan, H.; et al. Hungry Porphyrins: Protonation and Self-Metalation of Tetraphenylporphyrin on TiO2(110) - 1 × 1. *ChemistrySelect* **2016**, *1* (19), 6103−6105.
(21) Hötger, D.; Abufager, P.; Morchutt, C.; Alexa, P.; Grumelli, D.; Dreiser, J.; Stepanow, S.; Gambardella, P.; Busnengo, H. F.; Etzkorn, M.; et al. On-Surface Transmetalation of Metalloporphyrins. *Nanoscale* **2018**, *10* (45), 21116−21122.
(22) Franke, M.; Marchini, F.; Jux, N.; Steinrück, H. P.; Lytken, O.; Williams, F. J. Zinc Porphyrin Metal-Center Exchange at the Solid-Liquid Interface. *Chem. - Eur. J.* **2016**, *22* (25), 8520−8524.
(23) Cotton, T. M.; Schultz, S. G.; Van Duyne, R. P. Surface-Enhanced Resonance Raman Scattering from Water-Soluble Porphyrins Adsorbed on a Silver Electrode. *J. Am. Chem. Soc.* **1982**, *104* (24), 6528−6532.
(24) Verónica Rivas, M.; Méndez De Leo, L. P.; Hamer, M.; Carballo, R.; Williams, F. J. Self-Assembled Monolayers of Disulfide Cu Porphyrins on Au Surfaces: Adsorption Induced Reduction and Demetalation. *Langmuir* **2011**, *27* (17), 10714−10721.
(25) Cheung, S. K.; Dixon, F. L.; Fleischer, E. B.; Jeter, D. Y.; Krishnamurthy, M. Kinetic Studies of the Formation, Acid-Catalyzed Solvolysis, and Cupric Ion Displacement of a Zinc Porphyrin in Aqueous Solutions. *Bioinorg. Chem.* **1973**, *2* (4), 281−294.
(26) Lavallee, D. K. Complexation and Demetalation Reactions of Porphyrins. *Comments Inorg. Chem.* **1986**, *5* (3), 155−174.
(27) Bonnett, R. Metal Complexes for Photodynamic Therapy. In *Comprehensive Coord. Chem. II.*, McCleverty, J. A., Meyer, T. J., Eds.; Elsevier: Oxford, 2004; Vol. *9*, pp 945−1003.
(28) Funahashi, S.; Inada, Y.; Inamo, M. Dynamic Study of Metal-Ion Incorporation into Porphyrins Based on the Dynamic Characterization of Metal Ions and on Sitting-atop Complex Formation. *Anal. Sci.* **2001**, *17* (8), 917−927.
(29) Lexow, M.; Massicot, S.; Maier, F.; Steinrück, H. P. Stability and Exchange Processes in Ionic Liquid/Porphyrin Composite Films on Metal Surfaces. *J. Phys. Chem. C* **2019**, *123* (49), 29708−29721.
(30) Méndez De Leo, L. P.; de la Llave, E.; Scherlis, D.; Williams, F. J. Molecular and Electronic Structure of Electroactive Self-Assembled Monolayers. *J. Chem. Phys.* **2013**, *138* (11), 114707.
(31) Gouterman, M. Spectra of Porphyrins. *J. Mol. Spectrosc.* **1961**, *6*, 138−163.
(32) Hashimoto, T.; Choe, Y.-K.; Nakano, H.; Hirao, K. Chlorophylls, Theoretical Study of the Q and B Bands of Free-Base, Magnesium, and Zinc Porphyrins, and Their Derivatives. *J. Phys. Chem. A* **1999**, *103* (12), 1894−1904.
(33) Schneider, J.; Berger, T.; Diwald, O. Reactive Porphyrin Adsorption on TiO2 Anatase Particles: Solvent Assistance and the Effect of Water Addition. *ACS Appl. Mater. Interfaces* **2018**, *10* (19), 16836−16842.
(34) Ralphs, K.; Zhang, C.; James, S. L. Solventless Mechanochemical Metallation of Porphyrins. *Green Chem.* **2017**, *19* (1), 102−105.
(35) Baskin, J. S.; Yu, H. Z.; Zewail, A. H. Ultrafast Dynamics of Porphyrins in the Condensed Phase: I. Free Base Tetraphenylporphyrin. *J. Phys. Chem. A* **2002**, *106* (42), 9837−9844.
(36) Cai, J.; Chen, H.; Huang, J.; Wang, J.; Tian, D.; Dong, H.; Jiang, L. Controlled Self-Assembly and Photovoltaic Characteristics of Porphyrin Derivatives on a Silicon Surface at Solid-Liquid Interfaces. *Soft Matter* **2014**, *10* (15), 2612−2618.
(37) Diller, K.; Papageorgiou, A. C.; Klappenberger, F.; Allegretti, F.; Barth, J. V.; Auwärter, W. In Vacuo Interfacial Tetrapyrrole Metallation. *Chem. Soc. Rev.* **2016**, *45* (6), 1629−1656.
(38) Röckert, M.; Ditze, S.; Stark, M.; Xiao, J.; Steinrück, H. P.; Marbach, H.; Lytken, O. Abrupt Coverage-Induced Enhancement of the Self-Metalation of Tetraphenylporphyrin with Cu(111). *J. Phys. Chem. C* **2014**, *118* (3), 1661−1667.
(39) Wechsler, D.; Fernández, C. C.; Steinrück, H. P.; Lytken, O.; Williams, F. J. Covalent Anchoring and Interfacial Reactions of Adsorbed Porphyrins on Rutile TiO2(110). *J. Phys. Chem. C* **2018**, *122* (8), 4480−4487.
(40) Gárate-Morales, J. L.; Tham, F. S.; Reed, C. A. Do Sitting-atop Metalloporphyrin Complexes Exist? Observation of N-H- - -π Bonding in Arene Solvates of a Diprotonated Porphyrin Dication. *Inorg. Chem.* **2007**, *46* (5), 1514−1516.
(41) Lay, M. D.; Stickney, J. L. Electrodeposition of Au-Cd Alloy Nanostructures on Au(111). *J. Am. Chem. Soc.* **2003**, *125* (5), 1352−1355.
(42) Noyhouzer, T.; Mandler, D. Determination of Low Levels of Cadmium Ions by the under Potential Deposition on a Self-Assembled Monolayer on Gold Electrode. *Anal. Chim. Acta* **2011**, *684* (1−2), 1−7.
(43) Hammond, J. S.; Gaarenstroom, S. W.; Winograd, N. X-ray photoelectron spectroscopic studies of cadmium- and silver-oxygen surfaces. *Anal. Chem.* **1975**, *47* (13), 2193−2199.

https://dx.doi.org/10.1021/acs.langmuir.0c03197
Langmuir 2021, 37, 852−857